

# Highly Efficient One- and Two-Cascade Raman Lasers Based on Phosphosilicate Fibers

I. A. Bufetov<sup>1</sup>, M. M. Bubnov<sup>1</sup>, Y. V. Larionov<sup>1</sup>, O. I. Medvedkov<sup>1</sup>, S. A. Vasiliev<sup>1</sup>,  
M. A. Melkounov<sup>1</sup>, A. A. Rybaltovskiy<sup>1</sup>, S. L. Semjonov<sup>1</sup>, E. M. Dianov<sup>1</sup>, A. N. Gur’yanov<sup>2</sup>,  
V. F. Khopin<sup>2</sup>, F. Durr<sup>3</sup>, H. G. Limberger<sup>3</sup>, R.-P. Salathe<sup>3</sup>, and M. Zeller<sup>3</sup>

<sup>1</sup> Fiber Optics Research Center, A.M. Prokhorov General Physics Institute, Russian Academy of Sciences, ul. Vavilova 38, Moscow, 119991 Russia

e-mail: iabuf@fo.gpi.ru

<sup>2</sup> Institute of Chemistry of High-Purity Substances, Russian Academy of Sciences, ul. Tropinina 49, Nizhni Novgorod, 603600 Russia

<sup>3</sup> Institute of Applied Optics, Swiss Federal Institute of Technology, Lausanne, CH-1015 Switzerland

Received September 26, 2002

**Abstract**—Characteristics of one-cascade ( $1.06 \Rightarrow 1.24 \mu\text{m}$ ) and two-cascade ( $1.06 \Rightarrow 1.24 \Rightarrow 1.48 \mu\text{m}$ ) phosphorus-doped fiber Raman lasers are studied. The cavities of both lasers are formed by Bragg gratings written directly in the active fiber. Double-cladding  $\text{Yb}^{3+}$  and  $\text{Nd}^{3+}$  ion fiber lasers with  $\lambda \sim 1.06 \mu\text{m}$  were employed for pumping. These lasers were pumped, in their turn, by diode laser arrays with  $\lambda \sim 0.98 \mu\text{m}$  (Yb) and  $\lambda \sim 0.81 \mu\text{m}$  (Nd). The efficiency of the one-cascade laser with an unprecedentedly short length of 50 m was as high as 65% with 4.8-W pump radiation applied to the input of the laser. The maximum efficiency of the two-cascade Raman fiber laser was 40%. Gratings directly written in the active fiber reduced concentrated losses in laser cavities, which allowed the laser length to be decreased and the lasing threshold power of Raman fiber lasers to be lowered.

## 1. INTRODUCTION

Multicascade Raman fiber lasers (RFLs), created only in 1994 [1], are currently receiving numerous applications, mainly as pump sources for fiber-optic amplifiers in fiber communication lines.

Two types of optical fibers are being employed now as active media for the lasers of this class—fused silica single-mode fibers where the core is doped with either germanium dioxide (germanium-doped, or Ge-doped, fibers) or phosphorus pentoxide (phosphorus-doped, or P-doped, fibers). The choice of these fibers is dictated, on the one hand, by their Raman properties (the shape of the Raman gain spectrum) and, on the other hand, by the low magnitude of optical losses attainable with such fibers.

The modern level of Ge-doped fiber fabrication technologies allows extremely low optical losses to be achieved ( $\sim 0.25$  dB/km within the wavelength range around  $1.5 \mu\text{m}$ ). This factor is of special importance for Raman lasers in view of comparatively low Raman gains in these fibers [typically  $\sim 5$ – $10$  dB/(km W)]. Germanium-doped fibers possess a rather broad Raman gain band ( $\sim 100 \text{ cm}^{-1}$ ) and the Raman shift in the maximum of about  $440 \text{ cm}^{-1}$ . An additional refractive index can be also induced in the core of Ge-doped fibers [permitting refractive-index fiber Bragg gratings (FBGs) to be written] by UV laser radiation with wavelengths shorter than 400 nm. Bragg gratings may play the role of cavity mirrors in RFLs.

The minimum level of optical losses recently achieved for P-doped fibers is approximately two times higher than the level of losses attainable with Ge-doped fibers. However, the Raman spectrum of P-doped fibers has an additional, with respect to Ge-doped fibers, narrow band, shifted by  $1330 \text{ cm}^{-1}$  (which is approximately three times larger than the frequency shift in Ge-doped fibers, see Fig. 1). This circumstance allows the number of conversion cascades in a P-doped fiber Raman laser to be reduced as compared with the number of conversion cascades in a Ge-doped fiber Raman laser, which was demonstrated for the first time by Dianov *et al.* [2]. There are different ways to form optical cavities in P-doped fiber Raman lasers using FBGs. One of these approaches involves FBG writing in auxiliary segments of a germanium-doped fiber with a subsequent splicing of these segments with the active phosphorus-doped fiber. Such lasers have been implemented, in particular, by Karpov *et al.* [3]. However, the splicing regions in such RFL cavities give rise to additional optical losses, eventually lowering the laser efficiency. Still, this scheme allows high laser efficiencies to be achieved in certain situations [4].

Another approach is to write FBGs directly in a P-doped fiber segment serving as the active medium in an RFL. This method permits splicing losses inside RFL cavities to be completely avoided. However, FBG writing in the core of such fibers requires laser wavelengths shorter than 200 nm and an additional hydrogen processing of fibers before the irradiation [5]. Radiation

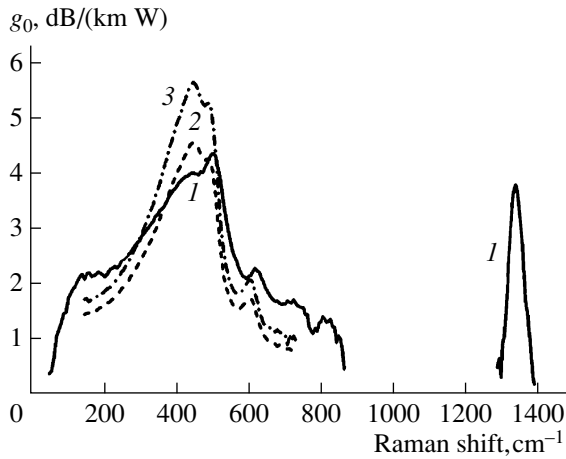


**Fig. 1.** The spectrum of Raman gain in optical fibers of different types (the pump wavelength is  $\lambda \sim 1.24 \mu\text{m}$ ): (1) phosphorus-doped fiber ( $\sim 10$  mol % of  $\text{P}_2\text{O}_5$ ), (2) large effective mode area fiber (LEAF), and (3) dispersion-shifted fiber (DSF).

of an ArF excimer laser ( $\lambda = 193 \text{ nm}$ ) is usually employed for this purpose. Most of ArF lasers available in research laboratories do not provide a sufficiently high beam quality (suffering from the low temporal and spatial coherence). Bragg gratings can be, therefore, efficiently written in this case only in a scheme with a phase mask [6], which substantially lowers the flexibility of the writing scheme with respect to the choice of the wavelength.

The possibility to avoid splicing losses in a P-doped fiber Raman laser cavity is, nevertheless, very attractive.

A one-cascade phosphorus-doped fiber laser with built-in FBGs, presented for the first time in [7], has demonstrated an unprecedentedly high efficiency with an active fiber length (200 m) much less than the active fiber lengths in lasers known from previously published results.

In this paper, we report the creation and investigation of a series of phosphorus-doped fiber Raman lasers without additional optical losses (with no splicing regions) in the laser cavity. We will demonstrate the possibility of creating a one-cascade laser as short as 50 m whose efficiency is close to the efficiency of the laser presented in [7]. A two-cascade phosphorus-doped fiber laser with built-in FBGs has been designed and implemented for the first time. Lasers with such a design are shown to provide a stable and high laser efficiency. Bragg gratings written in P-doped fibers processed with hydrogen and deuterium display different responses to the increase in the power of a two-cascade Raman laser.

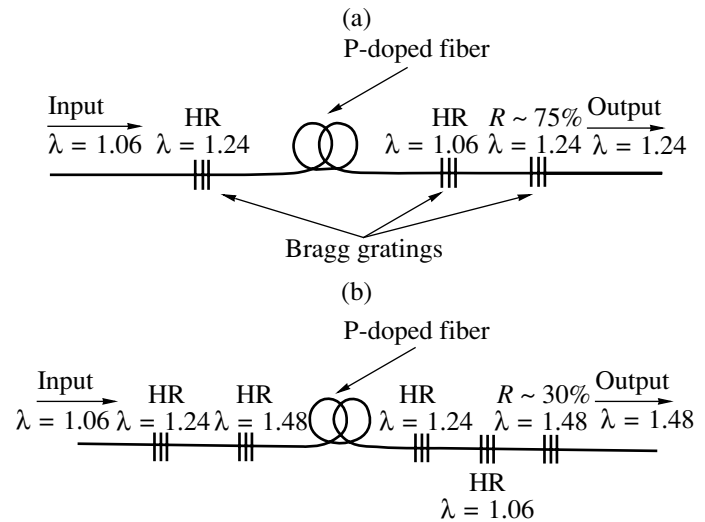


**Fig. 2.** Schemes of RFLs with FBGs written directly in a phosphorus-doped fiber: (a) one-stage RFL and (b) two-stage RFL; HR, Bragg grating with the reflection coefficient  $R = 99.9\%$ .

## 2. EXPERIMENTAL

One- and two-cascade RFL schemes studied in this paper are presented in Fig. 2.

Continuous-wave single-mode  $\text{Yb}^{3+}$  and  $\text{Nd}^{3+}$  double-cladding fiber lasers have been employed as pump radiation sources. The output radiation wavelength was about  $1.06 \mu\text{m}$ , and the output power reached  $5.5 \text{ W}$ . Pump radiation was coupled into a segment of a phosphorus-doped fiber with FBGs, playing the role of cavity mirrors, written at the ends of this fiber. An additional FBG with a reflection coefficient close to  $100\%$  (HR,  $\lambda = 1.06 \mu\text{m}$ ) was also written at the output of each scheme to return the unused fraction of pump radiation back to the cavity. The bandwidths of all the FBGs, except for the gratings serving as output couplers for the terminal RFL cascade, were  $\sim 1 \text{ nm}$ .

All the RFLs were created with the use of a fiber having the following parameters: the refractive-index step from the core to the cladding  $\Delta n = 0.01$ , the Raman gain at the wavelength of  $1.24 \mu\text{m}$   $g_0 = 7 \text{ dB}/(\text{km W})$ , the mode field diameter  $\text{MFD} = 5.7 \mu\text{m}$  at the wavelength of  $1.24 \mu\text{m}$ , the magnitude of optical losses at the pump wavelength  $\alpha = 1.44 \text{ dB}/\text{km}$ , the magnitudes of optical losses at the wavelengths of Stokes components employed in this work  $\alpha(\lambda = 1.24 \mu\text{m}) = 0.96 \text{ dB}/\text{km}$  and  $\alpha(\lambda = 1.48 \mu\text{m}) = 1.05 \text{ dB}/\text{km}$ . This fiber possessed a higher Raman gain and lower optical losses than the fiber used in [7], which had  $\alpha(\lambda = 1.24 \mu\text{m}) = 1.45 \text{ dB}/\text{km}$  and  $g_0 = 6.1 \text{ dB}/(\text{km W})$ .

We provide only approximate wavelengths for pump radiation, as well as the first and second Stokes components ( $1.06$ ,  $1.24$ , and  $1.48 \mu\text{m}$ ). These wavelengths slightly vary for different RFLs considered in

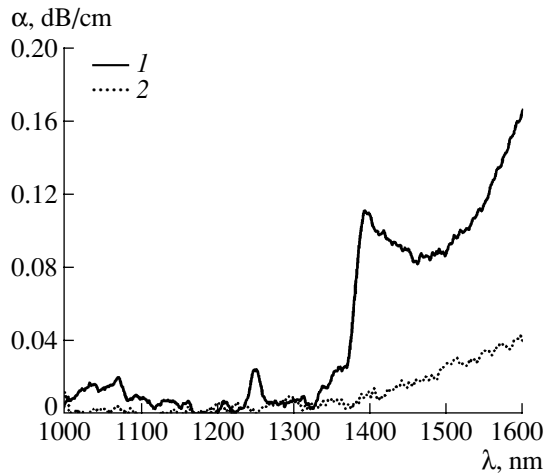


**Fig. 3.** The magnitude of optical losses ( $\alpha$ ) in a phosphorus-doped fiber irradiated with the UV light from an excimer ArF laser ( $\lambda \sim 193$  nm, the dose is  $2.16$  kJ/cm<sup>2</sup>) upon saturation with hydrogen or deuterium as a function of the wavelength: (1) fiber saturated with H<sub>2</sub> and (2) fiber saturated with D<sub>2</sub>.

this paper, and their values can be determined with a higher accuracy from the spectra presented below.

### 3. WRITING BRAGG GRATINGS

Bragg gratings were written in a P-doped fiber through a phase mask directly in the core of a phosphorus-doped fiber with the use of LPX-150 and CL-5000 ArF excimer lasers. Both lasers had unstable cavities. The energy density per pulse was equal to  $250$  mJ/cm<sup>2</sup> in the grating-writing scheme with the LPX-150 laser (with a pulse repetition rate of  $10$  Hz) and  $100$  mJ/cm<sup>2</sup> in the scheme with the CL-5000 laser (with a pulse repetition rate of  $20$  Hz).

All the Bragg gratings in one- and two-stage converters were written directly in an active fiber.

Before grating writing, P-doped fibers were saturated with gas deuterium or hydrogen at a temperature of  $100^\circ\text{C}$  and a pressure of about  $100$  atm during  $14$  h. Only P-doped fiber sections necessary for FBG writing (about  $5$  m from each side of the fiber) were saturated with hydrogen (deuterium). Upon grating writing, a fiber was kept in a climatic chamber at a temperature of  $\sim 80^\circ\text{C}$  during several days for hydrogen (deuterium) outflow.

It is well known that FBGs written in fibers saturated with hydrogen display strong absorption within the range of wavelengths exceeding  $1350$  nm due to OH groups produced under the action of UV light [8]. The adverse effect of this absorption is especially strong for the second cascade of the RFL, since this cascade generates output radiation with the wavelength of  $1.48$   $\mu\text{m}$ , falling within the spectral range where induced absorption is comparatively strong. Writing a

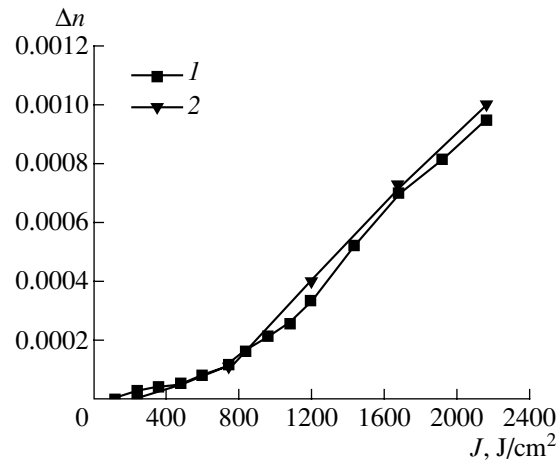


**Fig. 4.** The magnitude of the induced change in the refractive index  $\Delta n$  in a phosphorus-doped fiber saturated with (1) hydrogen and (2) deuterium as a function of the radiation dose  $J$ .

highly reflective grating, for example, requires a radiation dose of  $\sim 6$  kJ/cm<sup>2</sup>. The magnitude of absorption induced under these conditions at the wavelength of  $1.48$   $\mu\text{m}$  may reach  $0.1$  dB. Replacement of hydrogen by deuterium allows the magnitude of these optical losses to be reduced (see Fig. 3; spectra of induced losses similar to that presented in this figure have been also observed in earlier work [9]). The change in the refractive index achieved with different radiation doses, as shown in Fig. 4, is virtually the same for both technologies.

### 4. ONE-STAGE RAMAN FIBER LASERS

We studied parameters of two one-stage RFLs using segments of a phosphorus-doped fiber with a length of  $50$  m (1L1 laser) and  $250$  m (1L2 laser) as an active medium. The diagram of these lasers is presented in Fig. 2a. Bragg gratings were induced in both lasers in deuterium-saturated P-doped fibers.

The total power of radiation for all the wavelengths at the output of the system and the ratio of radiation powers at different wavelengths have been measured in our experiments. These results were then used to determine the dependences of the output power at the wavelengths of pump radiation (not absorbed in the RFL cavity) and RFL lasing  $\lambda = 1.24$   $\mu\text{m}$ . Radiation powers measured at the output of the RFL as functions of the pump power at the input of the system are presented in Fig. 5. For comparison, we present parameters of a P-doped fiber Raman laser with a similar design and a length of  $200$  m (1L3 laser) from [7]. Bragg gratings in the case of the 1L3 laser were recorded in a fiber processed with hydrogen rather than deuterium. Low threshold pump powers corresponding to RFL lasing,  $\sim 0.3$  W, indicate a high cavity finesse. The differential efficiency of first Stokes sideband generation was equal

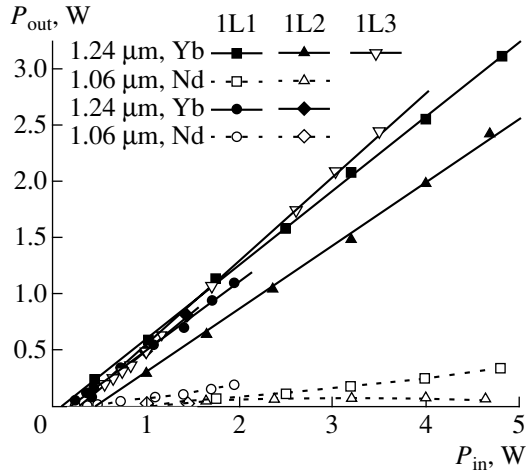


**Fig. 5.** Radiation power  $P_{out}$  at the output of one-cascade RFLs at the pump wavelength  $\lambda = 1.06 \mu\text{m}$  (transmitted radiation) and at the lasing wavelength  $\lambda = 1.24 \mu\text{m}$  as a function of the power  $P_{in}$  of the pump laser (Yb or Nd).

to 56% for 1L2 and 66% for 1L1, corresponding to differential quantum efficiencies of 66 and 77%, respectively.

The similarity of output characteristics of RFLs pumped with ytterbium and neodymium fiber lasers indicates that the coupling of RFL cavities and cavities of rare-earth ion lasers has no influence on lasing processes in the latter lasers. Slight deviations may be attributed to errors of measurements and small differences in the parameters of RFL gratings. Note that, in the case of RFLs pumped with either Nd or Yb lasers, nonstationary regimes of lasing were observed only with pump powers close to the threshold.

The RFL radiation spectrum considerably broadens as the pump power increases. Figure 6 displays the radiation spectra of the 1L1 laser for pump powers

equal to 0.5 and 4.8 W. For comparison, radiation spectra of the 1L3 RFL [7] corresponding to the pump powers equal to 1.2 and 3.5 W are presented. As can be seen from these data, with low pump powers, the RFL radiation spectrum does not fall beyond the limits of the FBG, and no dip is observed at the maximum of the line. For higher pump powers, the bandwidth increases, noticeably falling beyond the limits of the FBG. When the pump power reaches its maximum for each laser, the full width at half maximum (FWHM) of the spectral line exceeds 1 nm, becoming broader than the FBG reflection spectrum, and a clearly pronounced dip, corresponding to the position of the output FBG, shows up at the center of the output radiation spectrum. This spectral broadening can be apparently attributed to the joint action of four-wave mixing and stimulated Raman scattering [10]. This effect gives rise to additional radiation losses, reducing the conversion efficiency because of the lower spectral radiation density.

Note that the increase of the power in the cavity of one-cascade P-doped fiber Raman lasers is not accompanied by any shift of the FBG reflection spectrum (Fig. 6, FBG centers are shown by arrows), which indicates the low level of losses in gratings and is consistent with the dependence shown in Fig. 3.

### 5. TWO-STAGE RAMAN FIBER LASERS

We have created two two-stage RFLs (see Fig. 2b) with FBGs written by different methods. One of these lasers (denoted as 2L1) involved an FBG written with the use of hydrogen, while the second RFL (2L2) employed an FBG written with the use of deuterium.

Based on the results of numerical simulations, we chose the reflection coefficients of the output couplers equal to approximately 30%. The radiation powers at the output of two-stage RFLs as functions of the fiber-laser pump power are shown in Fig. 7. The differential

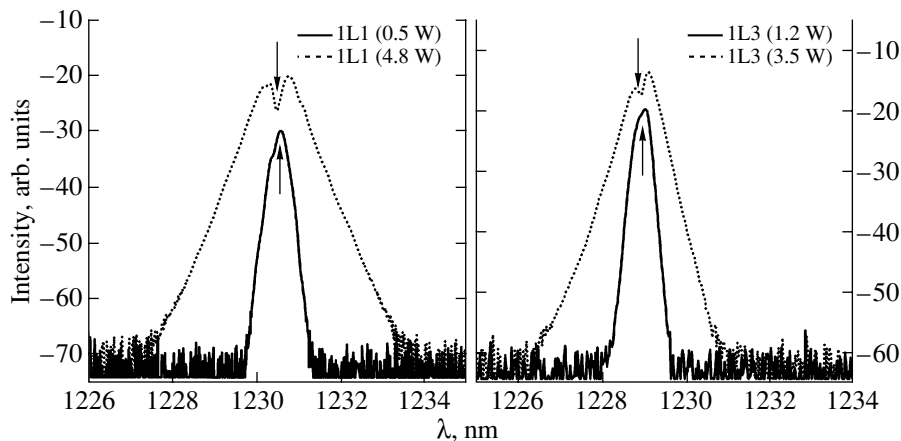


**Fig. 6.** Lasing spectra at the output of one-cascade RFLs for two pump powers. The arrows show the centers of reflection spectra of semitransparent FBGs.

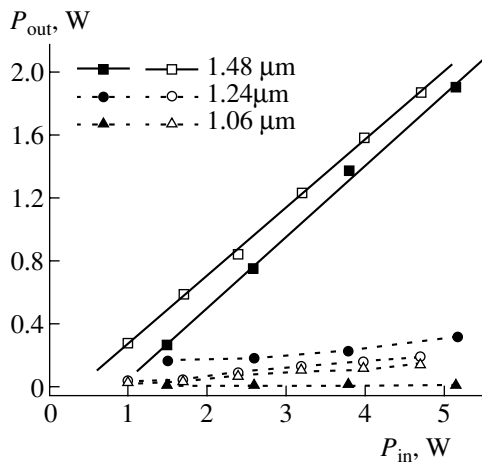


**Fig. 7.** Dependence of the radiation power  $P_{out}$  at the output of two-cascade RFLs on the power  $P_{in}$  of the pump laser (Yb) for radiation at the wavelengths  $\lambda = 1.48$ ,  $1.24$ , and  $1.06$   $\mu\text{m}$ .

efficiencies of both lasers in power were about 44%. However, the threshold power for the generation of the second Stokes component in the 2L2 laser is much lower, being equal to 0.5 W (1 W for the 2L1 laser),

while the total efficiency corresponding to the maximum available pump power ( $\sim 5$  W) is higher, reaching 40% (37% for 2L1). An even higher efficiency (45%) was achieved in our later work [11] with an RFL similar to 2L2, but using a P-doped fiber with a higher Raman gain [10 dB/(km W)] as an active medium. In spite of a certain increase in the magnitude of optical losses, the higher Raman gain ensured a better quality parameter of the laser (see [12]). The difference in the efficiencies achieved with 2L1 and 2L2 is apparently due to the higher losses in the FBGs of the former laser, produced in a hydrogen-saturated P-doped fiber. In spite of these differences, the RFL efficiencies for pump powers above 3 W are close to each other, regardless of the method used to process a P-doped fiber for FBG writing.

To examine the influence of splicing regions in the laser cavity, we performed an additional experiment. Upon measuring all the RFL parameters, we determined the efficiency of a laser (created using  $D_2$ ) with a special intracavity splicing, imitating a laser with spliced gratings. The efficiency lowered from 43 down to 29% under these conditions. Such a substantial decrease in the efficiency was associated with the high magnitude of losses ( $>0.2$  dB) in the splicing region. Kurkov *et al.* [4] have achieved a high efficiency

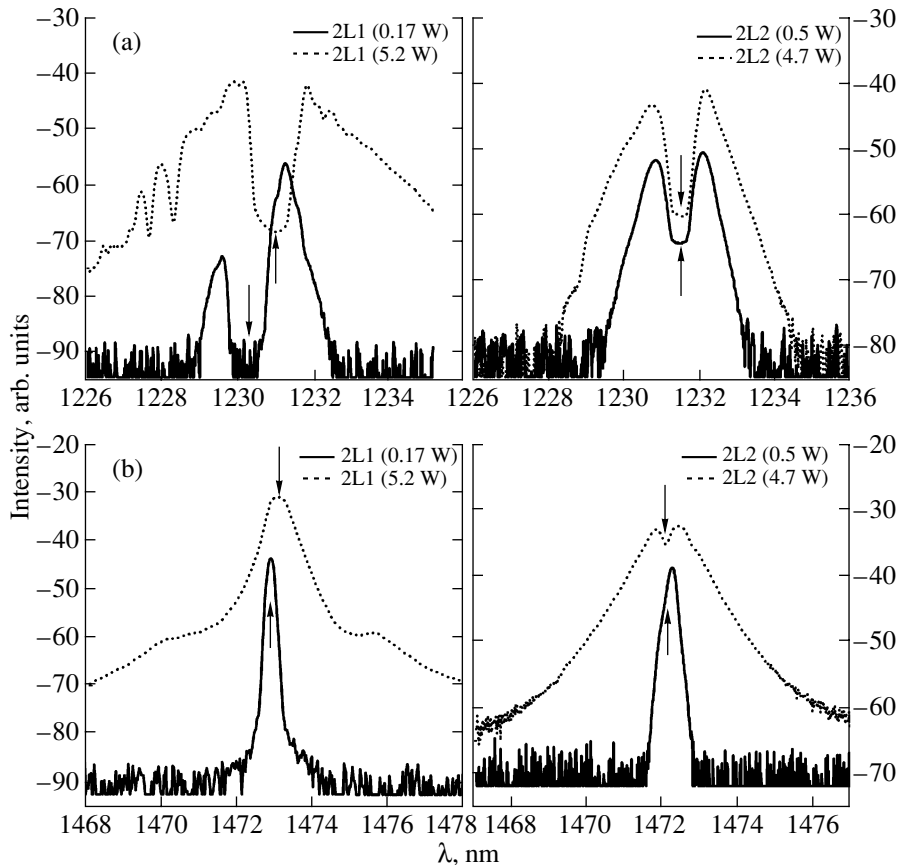


**Fig. 8.** Lasing spectra at the output of two-cascade RFLs at the wavelengths of (a) the first and (b) second cascades for two pump powers. The arrows show the centers of reflection spectra of FBGs at the output of the RFL.

(42.5%) with a two-stage P-doped fiber Raman laser with spliced gratings. Apparently, this result was obtained due to the high quality of FBG–fiber splicing.

Note that, similar to the case of one-cascade RFLs, two-cascade lasers display spectral broadening of each component, although in the idealistic case of no broadening, the intermediate component should saturate right above the lasing threshold power in the second cascade. Figure 8 presents radiation spectra at the output of an RFL for the first and second cascades of both two-cascade lasers with two different pump powers. The central dips in these spectra correspond to a totally reflecting (Fig. 8a) and a semitransparent (Fig. 8b) output gratings for each cascade. As can be seen from these data, the output radiation spectra for both cascades of the laser created with the use of deuterium display virtually no shift in the wavelength, but only broaden (the FBG centers are shown by arrows) at the maximum pump power, while the radiation spectra of the RFL created with the use of H<sub>2</sub> display a noticeable red shift (by ~0.7 nm in the first cascade and by ~0.3 nm in the second cascade) with the growth in the power. Such a shift in the FBG position is observed when an FBG is placed in air without additional cooling. When an FBG was placed in a liquid (glycerol) for better heat removal, the maximum shift (0.7 nm) was reduced to 0.2 nm. Apparently, the FBG shift, accompanying the increase in the power generated at  $\lambda = 1.48 \mu\text{m}$ , is due to higher losses in gratings written in a hydrogen-saturated fiber. Gratings are heated under these conditions, and their reflection spectrum becomes red-shifted. All the FBGs located to the right of the active fiber in Fig. 2b and one FBG (HR,  $\lambda = 1.48 \mu\text{m}$ ) located to the left of the active fiber are subject to the influence of radiation with the wavelength  $\lambda = 1.48 \mu\text{m}$ . The shifts of highly reflective gratings are larger than the shifts of semitransparent gratings, since the former gratings are characterized by higher losses because of the higher radiation dose. The temperature required to shift the reflection spectrum of a grating by 0.7 nm to the right along the wavelength axis is on the order of 70°C. Note that the wavelength shifts of FBGs were observed only for two-stage RFLs. Virtually no FBG shifting was observed for one-cascade RFLs (see Fig. 6). This finding supports the hypothesis that optical losses in FBGs of the RFLs under study are mainly due to absorption at the wavelength of 1.48  $\mu\text{m}$  induced by UV radiation in the process of FBG writing (Fig. 3).

## 6. CONCLUSION

In this study, we have measured characteristics of one- and two-cascade phosphorus-doped fiber Raman lasers with Bragg gratings written directly in the active fiber preprocessed with hydrogen or deuterium. Two-cascade lasers with Bragg gratings written directly in P-doped fibers were implemented for the first time in this work. Gratings directly written in the active fiber allowed the concentrated intracavity losses to be substantially lowered, thus permitting the length of the active part of the laser to be reduced and the lasing threshold to be decreased, offering the way for creating stable RFLs with a high efficiency.

For the one-cascade RFL with output radiation at 1.24  $\mu\text{m}$  with an unprecedentedly short, 50-m active fiber, the differential efficiency of 66% and the lasing threshold less than 0.3 W have been achieved. For two-cascade RFLs, the differential efficiency was about 44%. The two-cascade laser created with the use of deuterium had a higher total efficiency and a lower threshold power required for the generation of the second Stokes component with respect to an identical laser with FBGs written with the use of hydrogen. With the increase of the power inside the cavity, we observed a red shift in the spectral position of gratings produced in a hydrogen-saturated fiber.

## REFERENCES

1. Grubb, S.G., Erdogan, T., Mizrahi, V., *et al.*, 1994, *Opt. Ampl. Appl.* (Breckenridge), PD-3.
2. Dianov, E.M., Grekov, M.V., Bufetov, I.A., *et al.*, 1997, *Electron. Lett.*, **33**, 1542.
3. Karpov, V.I., Dianov, E.M., Kurkov, A.S., *et al.*, 1999, *OFC'99* (San Diego, USA), WM3-1.
4. Kurkov, A.S., Kurukitkoson, N., Sugahara, H., *et al.*, 2001, *ECOC 2001* (Amsterdam, Netherlands), p. 176.
5. Malo, B., Albert, J., Bilodeau, F., *et al.*, 1994, *Appl. Phys. Lett.*, **65**, 394.
6. Hill, K.O., Malo, B., Bilodeau, F., *et al.*, 1993, *Appl. Phys. Lett.*, **62**, 1035.
7. Dianov, E.M., Bufetov, I.A., Bubnov, M.M., *et al.*, 1999, *OFC'99* (San Diego, USA), PD25.
8. Semjonov, S.L., Rybaltovsky, A.A., Dianov, E.M., *et al.*, 2000, *OSA TOPS*, **33**, 267.
9. Stone, J., 1987, *J. Lightwave Technol.*, **LT-5**, 712.
10. Karpov, V.I., Clements, W.R.L., Dianov, E.M., and Papernyi, S.B., 2000, *Can. J. Phys.*, **78**, 407.
11. Bufetov, I.A., Bubnov, M.M., Larionov, Y.V., *et al.*, 2002, *CLEO'2002* (Long Beach, Cal.), CThJ5.
12. Bufetov, I.A. and Dianov, E.M., 2000, *Quantum Electron.*, **30**, 873.